Phonons and fractons in sol-gel alumina: Raman study

ANUSHREE ROY and AJAY K SOOD*

Department of Physics, Indian Institute of Science, Bangalore 560012, India
*Also at Jawaharlal Nehru Centre for Advanced Scientific Research, Jakkur Campus, Bangalore 560064, India

Abstract. We report Raman scattering from the boehmite, γ-, δ- and α-phases of the alumina gel. Samples are characterized by transmission and scanning electron microscopy, X-ray diffraction and density measurements. The main Raman line in the boehmite phase is red-shifted as well as asymmetrically broadened with respect to that in the crystalline boehmite, signifying the nanocrystalline nature of the gel. Raman signatures are absent in the γ- and δ-phases due to the disorder in cation vacancies. We also show that low frequency Raman scattering from the boehmite phase resembles that from a fractal network, characterized in terms of fraction dimension $\tilde{d}$. Taking Hausdorff dimension D of the boehmite gel to be 2·5 (or 3·0), the value of $\tilde{d}$ is 1·33 $\pm$ 0·02 (or 1·44 $\pm$ 0·02), which is close to the theoretically predicted value of 4/3.

1. Introduction

In recent years there has been a considerable interest in static and dynamic properties of random systems, such as gels and glassy networks. The sol-gel route of preparation of porous transparent alumina gel (Al-gel) was first established by Yoldas [1]. It is a three-step process: (i) hydrolysis and condensation of aluminium alkoxide in excess water to form AlO(OH) precipitate (ii) peptization of the hydroxide to clear the sol and (iii) concentration of the sol by slow evaporation of the solvent resulting in gel formation. It has been shown [2] that the morphology and structure of aluminium hydroxide gels prepared from aluminium-sec-butoxide under acidic conditions depend crucially on temperature. The gels formed by the peptization of the sol with an acid above 50°C termed as high temperature gels, show presence of nanocrystalline platelets. On the other hand, whenever all the chemical processing is performed at room temperature, the structure of the gel is termed as 'super amorphous' as studied by X-ray diffraction. In this paper we will discuss the structure and vibrational properties of the high temperature alumina hydrogel, boehmite γ-AlO(OH), and its other phases formed by the transformation sequence

$$\gamma\text{-AlO(OH)} \to \gamma\text{-Al}_2\text{O}_3 \to \delta\text{-Al}_2\text{O}_3 \to \alpha\text{-Al}_2\text{O}_3.$$
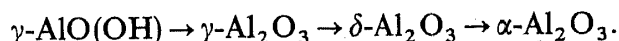
The structure of crystalline boehmite is orthorhombic [3,4] with two AlO(OH) units per primitive unit cell. The structure consists of extended layers perpendicular to the b-axis [4]. Each layer has two planes of aluminium atoms and four planes of oxygen atoms. Each aluminium atom is bonded with six oxygen atoms in a distorted

octahedron. The oxygen atoms present in the inner planes are each bonded with four aluminium atoms in a highly distorted tetrahedron. The outer plane oxygen atoms are each bonded to only two aluminium atoms. The intralayer interactions between atoms are through covalent and ionic bonding, whereas hydrogen bonding is present between the layers. A transformation from boehmite to the dehydroxylated alumina γ-phase, γ-Al_2O_3, occurs at $\sim 400°C$ when water is expelled from boehmite resulting in collapse of the layers and the cubic structure is formed as a result of rearrangement of the oxygen atoms. The γ-Al_2O_3 has a defect spinel structure (A_2BO_4) in which A^{3+} ions are octahedrally coordinated to O^{2-} ions, while B^{2+} ions have tetrahedral coordination to the anions [5]. The oxygen atoms are in an almost perfect cubic close-packing with metal atoms lying in the holes of the packing. In γ-Al_2O_3 structure, the cation vacancies are assumed to be disordered among the octahedral and tetrahedral sites with the probability of the occupation of the vacancies in the tetrahedral sites being more by a factor of 2/3 than in the octahedral sites. The γ-Al_2O_3 to δ-Al_2O_3 phase transformation occurs at $\sim 800°C$. In δ-Al_2O_3 the vacancies are ordered on octahedral sites, giving it a spinel superstructure [6]. The transformation of δ-Al_2O_3 to α-Al_2O_3 phase occurs at $\sim 1200°C$. The structure of α-Al_2O_3 is rhombohedral and belongs to a space group D_{3d}^6 with two molecular Al_2O_3 per unit cell [7]. In α-Al_2O_3 the aluminium atoms are coordinated with two layers of oxygen atoms in distorted octahedra [8].

The high temperature boehmite gel is composed of nanocrystalline platelets with an average size of $\sim 60 Å$ [1] and a narrow size distribution, which are somewhat ordered like in a smectic array [6]. The gel is highly porous (porosity ~ 60–70%) [1]. The dehydration of the boehmite to γ-Al_2O_3, δ-Al_2O_3 and α-Al_2O_3 represents topotactic deformation of the network (i.e. the crystal structures are accomplished without any change in crystalline morphology) and is accompanied by changes in the morphology of the porosity [9]. Wilson and Stacey [9] showed that the microstructure characteristic of γ-Al_2O_3 consists of a system of fine lamellar pores which are perpendicular to the planes of the boehmite platelets. Their orientation and spacing are quite regular with some evidence of extensive cross-linking. The pores take a planar hexagonal shape. In δ-Al_2O_3, the pores have the same morphology as in γ-Al_2O_3 but merged into larger hexagonal planar pores of several hundred angstroms. The average pore size increases with further heat treatment. In α-Al_2O_3, monocrystals with wormy texture [6] entrapping a high proportion of pores can be seen. Thus in spite of topotactic transformation, each stage of the transformation sequence has a characteristic microstructure due to the variations in the pores morphology.
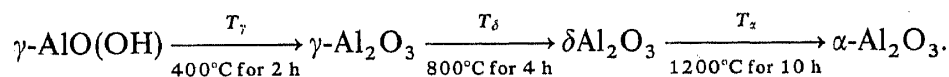
Motivated by the above observations on wide variation of microstructure of different phases of Al-gel, we have studied the vibrational properties of such structures (characterized using X-ray diffraction) by Raman scattering. While this work had been almost completed, we learnt of a recent paper on Raman studies of the nanocrystalline boehmite phase of the Al-gel [4]. In this paper, we present results on the Raman scattering from the phonons in the different phases of the Al-gel and compare them with the known results in the literature. We have also studied, for the first time, the low frequency $(20$–$300\,cm^{-1})$ Raman intensity which is known to give information about the dynamics of the fractal network—for example that of the silica gel [10] and the porous silicon [11]. It has been shown that the fracton dimension $\tilde{d}$ which characterizes vibration density of states of the fractal network, $g(\omega) \sim \omega^{(\tilde{d}-1)}$, can be determined from the Raman intensity in the low frequency range. Our experimental

results do suggest that dynamics of the boehmite phase of the Al-gel has characteristics that of a fractal network below a certain length scale.

Section 2 gives the experimental details and the results along with their discussion are given in § 3.

2. Experimental

Hydrolysis of aluminium isopropoxide $Al(OC_3H_7)_3$ was performed in excess deionized water under vigorous stirring for 15–20 min at 80°C. For peptization, 12N hydrochloric acid was added as catalyst into the slurry kept at 90°C for about 25 min. The alkoxide to water to acid molar ratio was kept at 1:100:0·3 having pH of the solution ~ 3. The sol-gel transition occurs by slow evaporation of the solvent at room temperature for at least 48 h. The boehmite hydrogel was transformed to the other phases by heating it in air for fixed temperatures ranging from 125°C to 1200°C [12]. The transition temperature, T_γ, for γ-phase was 400°C and that for δ-phase, T_δ, was 800°C. The α-Al_2O_3 was formed by heating δ-phase at 1200°C for 10 h (T_α). In summary, the dehydration sequence of Al-gel is as follows:

$$\gamma\text{-AlO(OH)} \xrightarrow[\text{400°C for 2 h}]{T_\gamma} \gamma\text{-Al}_2\text{O}_3 \xrightarrow[\text{800°C for 4 h}]{T_\delta} \delta\text{Al}_2\text{O}_3 \xrightarrow[\text{1200°C for 10 h}]{T_\alpha} \alpha\text{-Al}_2\text{O}_3.$$

X-ray diffraction of the powdered samples is obtained at room temperature using Philip's diffractometer, model PW 1050/70 equipped with a vertical goniometer and CuK_α radiation (wavelength $\lambda = 1\cdot514$ Å). The scanning and transmission electron microscopy are performed using Cambridge S360 and JEOL 2000CX instruments, respectively. The electron micrographs of the different phases are similar to the reported results [6,9]. The density of the boehmite gel measured was 2·38 g/cc. Comparing this with the density of 3·01 g/cc for the crystalline boehmite indicates a porosity of 20% in the gel with respect to the crystalline boehmite. The densities of the γ-, δ- and α-phases are 3·19, 3·45 and 3·87 g/cc, respectively. The Raman spectra are recorded at room-temperature using Dilor X-Y spectrometer equipped with a liquid nitrogen cooled CCD detector and 5145 Å radiation from an argon ion laser (power ~ 100 mW).

3. Results and Discussion

3.1 *X-ray diffraction*

X-ray diffraction patterns of the four different phases of Al-gel are shown in figure 1. The observed value of diffraction angles (2θ) for all the phases matches quite well with the reported data [13]. Analysis of X-ray diffraction patterns confirms the nanocrystalline structure of the boehmite gel. The peak assignment for the boehmite phase can be given with respect to the orthorhombic structures of its corresponding crystalline phase [3,14]. The large linewidth is due to the finite size of the crystallites in the gel. The crystallite size, L, can be calculated from the full width at half maxima (FWHM), Γ (expressed in radians), of the X-ray diffraction peak using Scherrer's equation [15]

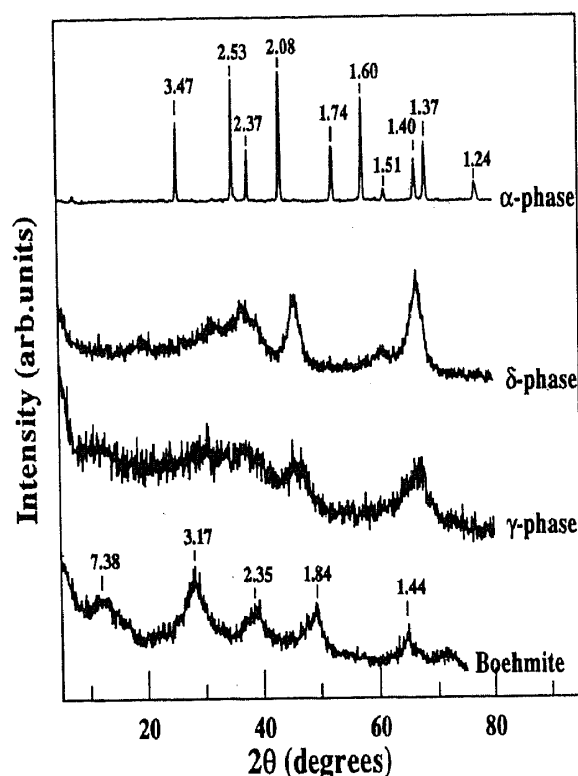$$\Gamma = \frac{0\cdot94\lambda}{L\cos\theta}, \tag{1}$$

Figure 1. X-ray diffraction pattern for the different phases of alumina gel.

where θ is the diffraction peak position. Taking the diffractometer resolution function (DRF) to be Gaussian and the diffraction line to be Lorentzian, the linewidth correction for the X-ray instrumental broadening can be taken into account by using the empirical expression [16]

$$\eta = \eta_e - (1/\eta_e)^{\beta},\qquad\qquad(2)$$

where $\beta = 1 - 0.1107/\eta_e$. The η_e is the ratio of observed FWHM (Γ_e) and the FWHM (Γ_d) of the DRF. The η is the ratio of the true FWHM (Γ) of the diffraction line and Γ_d. Γ_d is equal to $0.53°$ for our instrument. For the diffraction peak at $2\theta = 28°$ of the boehmite gel, $\Gamma_e = 1.73°$ which gives $\Gamma = 1.56°$ and hence the crystallite size can be estimated from (1) to be 55 Å. For γ- and δ-phases of alumina, the diffraction lines are much broader. These broad X-ray lines can arise due to considerable disorder as expected from their structure containing cation vacancies [5]. The α-Al_2O_3 phase shows sharp X-ray diffraction lines which confirms the high crystalline order of this phase and the values of the lattice spacings agree with that of the corundum structure [17]. The results of indexing for the boehmite and the α-Al_2O_3 have been summarized in tables 1 and 2, respectively.

3.2 Raman spectra: Phonons

Raman spectra of different phases of the Al-gel are shown in figure 2. We shall analyse the spectra in the context of their crystalline counterparts. The Al-O optical vibrational modes in crystalline boehmite can be classified according to the irreducible

Table 1. Reported d-values of the crystalline boehmite $(d_{x-boehmite})$ for some (hkl) values and d-values obtained from the powder diffraction pattern of boehmite gel (d_{gel}).

(hkl)	$d_{x-boehmite}$	d_{gel}
071	1·49	1·44
160	1·78	1·84
111	2·29	2·45
040	3·05	3·17

Table 2. Reported d-values of the corundum $(d_{corundum})$ and d-values as obtained from powder diffraction pattern of α-Al_2O_3 phase of the alumina gel $(d_{\alpha-Al_2O_3})$. The relative intensity of each diffraction line of corundum also has been listed with its corresponding (hkl) value.

hkl	Intensity	$d_{corundum}$	$d_{\alpha-Al_2O_3}$
012	75	3·48	3·47
104	90	2·55	2·53
110	40	2·38	2·37
113	100	2·09	2·08
024	45	1·74	1·74
116	80	1·60	1·60
018	8	1·51	1·51
124	30	1·40	1·40
030	50	1·37	1·37
1·0·10	16	1·24	1·24

representations of space group D_{2h}^{17} [18]

$$\Gamma_{Al-O} = 3A_{1g}^R + 3B_{1g}^R + 3B_{2g}^R + 2B_{1u} + 2B_{2u} + 2B_{2u},$$

in which only A_{1g}, B_{1g} and B_{2g} modes are Raman active. The observed Raman peak positions in crystalline boehmite are 676, 497 and 369 cm^{-1} for the A_{1g} modes (which are the most intense); 639, 272 and 232 cm^{-1} for the B_{1g} modes and 454, 343 and 260 cm^{-1} for B_{2g} modes. Raman spectra of the boehmite gel shows only the intense A_{1g} modes [figure 2]. The inset of figure 2 shows the expanded plot of the 359 cm^{-1} mode to bring out the asymmetric and broad lineshape with a shift in peak position towards the lower energy as compared to that of the crystalline boehmite. Such a broadening, asymmetry and peak shift (of ~ 10 cm^{-1}) of the Raman mode compared to that of the bulk crystalline boehmite can be attributed to the effect of phonon confinement as observed in the nanostructure of semiconductors [19–21]. In nanocrystallites, phonon can no longer be described by a plane wave but rather by a wave packet whose spatial dimensions are comparable to the crystallite size. This introduces a spread in the wavevector (proportional to the inverse of the particle size) as expected from the uncertainty principle. Since the optic phonon dispersion curves
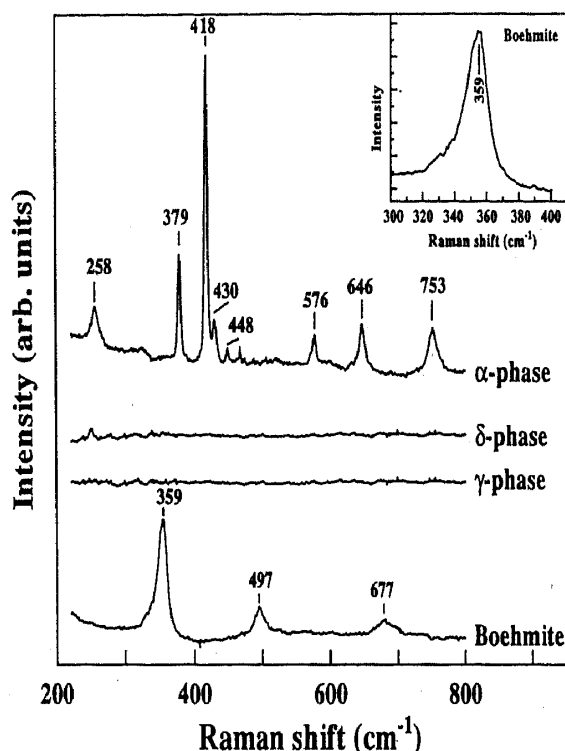
Figure 2. Raman spectra of the different phases of alumina gel.

of the bulk crystal usually bend towards lower frequency for nonzero wavevectors, an integration of the Lorentzian lineshape over the wavevector gives rise to a shift and an asymmetry of the Raman lines towards lower frequency side [19]. A quantitative analysis of the $359\,cm^{-1}$ line shape (shown in the inset) in terms of the phonon confinement model will require the average dispersion curve of the crystalline boehmite, which is not yet available.

As shown in figure 2, Raman lines are absent in γ- and δ-phases. This interesting result can be understood as follows. Among all the vibrational modes for a regular spinel structure A_2BO_4, to which γ- and δ-phases are related, the only *Raman active vibrations* are the internal modes of *tetrahedral* BO_4 groups, whereas octahedral group vibrations are Raman inactive. In γ- and δ-phases cation vacancies are preferentially situated on the tetrahedral sites and the number of tetrahedrally coordinated Al^{3+} ions is a minor fraction compared to that of the octahedrally coordinated Al^{3+} ion. This can explain the absence of Raman lines in the γ- and δ-phases [22].

The irreducible representations for the optical modes in the α-Al_2O_3 crystal of space group D_{3d}^6 are

$$2A_{1g}^R + 5E_g^R + 2A_{1u} + 3A_{2g} + 2A_{2u} + 2E_u.$$

Among all these modes, only seven vibrations $2A_{1g} + 5E_g$ are Raman active. The Raman peaks in α-phase occur at 379, 418, 430, 448, 576, 646 and $753\,cm^{-1}$. These are the same as in the corundum phase [23], where the modes at 418 and $646\,cm^{-1}$ correspond to the A_{1g} symmetry and modes at 379, 430, 448, 576 and $753\,cm^{-1}$ belong to the E_g symmetry. The origin of the peak at $258\,cm^{-1}$ is not clear at present.

3.3 *Fractons*

The vibrational modes in a disordered system can be localized in contrast to the propagating phonon states in crystalline materials. This localization can be a consequence of scattering (analogous to Anderson localization) or it can be geometric in origin as on a fractal network. For the latter, it has been shown that the vibrational density of states changes from the Debye form to a power law, $g(\omega) \sim \omega^{(\tilde{d}-1)}$ where $\tilde{d}$ is called the fracton dimension. These fracton modes can show up in low frequency Raman scattering experiments where the scattered intensity $I(\omega)$ by fraction modes obey the equation [10, 24]

$$\frac{I(\omega)\omega}{[n(\omega)+1]} \propto \omega^{\nu},\qquad (3)$$

where

$$\nu = \frac{\tilde{d}(2d_\phi + D)}{D} - 1.\qquad (4)$$

Here $[n(\omega)+1]$ is the usual Bose–Einstein factor, d_ϕ is the geometrical exponent describing the localization of the fractons in real space and D is the fractal Hausdorff dimension. The fractons are spatially localized for $\tilde{d} < 2$. Experimental determination of ν yields the fracton dimension $\tilde{d}$ of the fractal structure for a given value of D and d_ϕ. It has been demonstrated that the low frequency Raman scattering in the silica gel having a fractal morphology does obey (3). Figure 3 shows our data for the Raman scattering from the silica gel. From log-log plot of $I(\omega)\omega/[n(\omega)+1]$ vs ω, the slope ν obtained from the least square fit is $1\cdot35 \pm 0\cdot03$ [figure 3] which is very close to $1\cdot39$ reported before [10]. Taking $D = 2\cdot5$ (or $3\cdot0$) and $d_\phi = 1$ the value of $\tilde{d}$ comes to be equal to $1\cdot31 \pm 0\cdot02$ (or $1\cdot41 \pm 0\cdot02$).

Motivated by the results on the silica gel, we have carried out Raman measurements from $\omega > 20\,\text{cm}^{-1}$ on the clear platelet samples of the boehmite, γ- and δ- phases. Inset of figure 3 shows the $\log I(\omega)\omega/[n(\omega)+1]$ vs $\log \omega$ for HV polarization for different phases of Al-gel in the spectral range of $50\,\text{cm}^{-1}$ to $200\,\text{cm}^{-1}$. It is clear from the inset of figure 3, that only the plot for the boehmite phase of Al-gel can be fitted by a straight line, obeying (3). In figure 3 we show $\log I(\omega)\omega/[n(\omega)+1]$ vs $\log \omega$ plot for the boehmite gel both in HV and VV polarization. The depolarization ratio is $0\cdot7$. The least square fit to the experimental data has been shown by bold straight lines to yield $\nu = 1\cdot41 \pm 0\cdot03$ for HV and $\nu = 1\cdot46 \pm 0\cdot03$ for VV polarization. So far, there is no small angle X-ray or neutron scattering measurements of the boehmite gel to give the fractal dimension D. We can take D to be $2\cdot5$ as in silica gel [10]. It can be seen from (4) that the value of $\tilde{d}$ is not very sensitive to the value of D. Using (4), and taking $\nu = 1\cdot41$, $d_\phi = 1$ (same as in silica gel) and $D = 2\cdot5$, we get the fracton dimension, $\tilde{d}$, of boehmite phase to be equal to $1\cdot33 \pm 0\cdot02$. This measured value of $\tilde{d}$ is surprisingly close [25] to the theoretical prediction of $4/3$. The experimental coefficient $\nu = 1\cdot41$ fits the experimental data for frequencies higher than $\omega_{\text{min}} \sim 50\,\text{cm}^{-1}$. This means the fractal regime is effective at length scales [24] shorter than $L_f \sim v_{\text{sound}}/c\,\omega_{\text{min}}$, where v_{sound} is the speed of acoustic phonon in the medium and c is the speed of light. Taking $v_{\text{sound}} = 10 \times 10^5\,\text{cm/s}$ for alumina gel and $\omega_{\text{min}} = 50\,\text{cm}^{-1}$, L_f calculated is $70\,\text{Å}$.
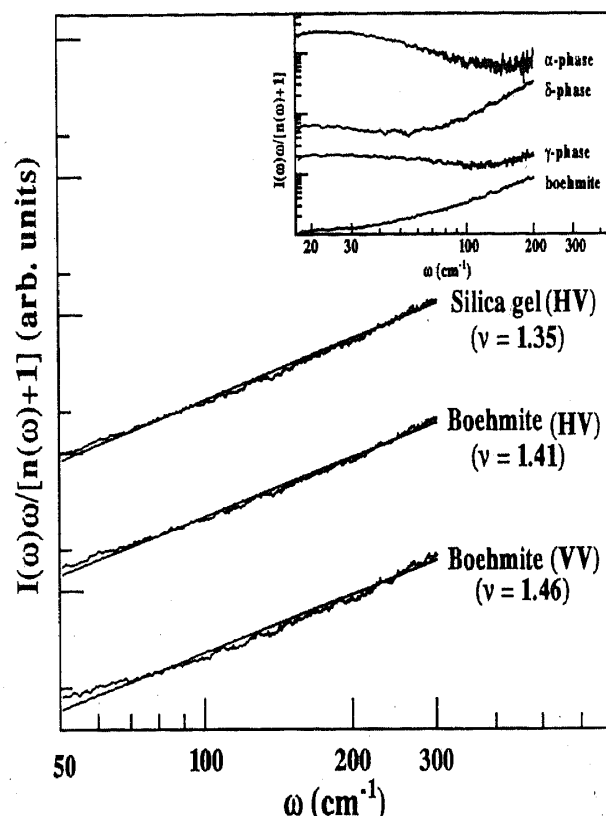
Figure 3. Log-log plot of $I(\omega)\omega/[n(\omega) + 1]$ vs ω for ω between 50 and 200 cm^{-1} for the silica gel and the boehmite phase of the alumina gel. For the boehmite phase the plots for both polarization VV and HV are shown. The slope v (eq. 3) has been marked for each case. Inset shows the plot for the different phases of the alumina gel.

4. Conclusions

We see that in spite of topotactic transformation of the Al-gel, each of its phases has different vibrational characteristics and different microstructure due to the variation in morphology of porosity. The main Raman line in the boehmite gel phase is red shifted and asymmetrically broadened with respect to the corresponding line in the crystalline boehmite, indicating the nanocrystalline nature of the gel. The absence of Raman lines in the γ- and δ-phases is attributed to preferential occupation of the octahedral sites in the spinel structure by Al^{3+} ions. Our low frequency Raman data suggest that the pore morphology in the boehmite alumina gel can be best characterized in terms of fractals below a certain length scale of ~ 70 Å. It would be very interesting to carry out small angle neutron and X-ray scattering measurements to measure the fractal Hausdorff dimension D.

References

[1] B E Yoldas, *Am. Ceram. Soc. Bull.* **54**, 286 (1975)

[2] A C Pierre and D R Uhlmann, *J. Non-Cryst. Solids* **82**, 271 (1986)

[3] C E Corbato, R T Tettenhorst and G G Christoph, *Clays clay Miner* **33**, 71 (1985)

[4] C J Doss and R Zallen, *Phys. Rev.* **B48**, 15626 (1993)

[5] M I Baraton and P Quintard, *J. Mol. Struct.* **79**, 337 (1982)

[6] X Yang, A C Pierre and D R Uhlmann, *J. Non-Cryst. Solids* **100**, 371 (1988)

[7] R W G Wyckoff, *Crystal structures* (Interscience Publishers, Inc., New York, 1948) vol 2

[8] S Geschind and S J P Remeika, *Phys. Rev.* **122**, 757 (1961)

[9] S J Wilson and M H Stacey, *J. Colloid, Interface Sci.* **82**, 507 (1981)

[10] A Boukenter, B Champagnon, E Duval, J Dumas, J F Quinson and J Serughetti, *Phys. Rev. Lett.* **57**, 2391 (1986)

[11] A Roy and A K Sood, *Solid State Commun.* **93**, 995 (1995)

[12] V Saraswati, G V N Rao and G V Rama Rao, *J. Mater. Sci.* **22**, 2529 (1987)

[13] B C Lippens and J H de Boer, *Acta Crystallogr.* **17**, 1312 (1964)

[14] G G Christoph, C E Corbato, D A Hofmann and R T Tettenhorst, *Clays Clay Miner.* **27**, 81 (1979)

[15] B E Warren, *X-ray diffraction* (Addison-Wesley, Reading, MA, 1969) pp. 253 and 258 H P Klug and L E Alexander, *X-ray diffraction procedures for polycrystalline and amorphous materials* (Wiley, New York, 1973) pp. 687 and 635

[16] A K Arora and V Umadevi, *Appl. Spectrosc.* **36**, 424 (1982)

[17] Powder diffraction file (International Centre for Diffraction Data, 1990) 10–173

[18] A B Kiss, G Keresztury and L Farkas, *Spectrochim. Acta* **A36**, 653 (1980)

[19] I H Campbell and P M Fauchet, *Solid State Commun.* **58**, 739 (1986)

[20] P M Fauchet and I H Campbell, *Critical review in solid state and materials sciences* **14**, S79 (1988)

[21] Anushree Roy, K Jayaram and A K Sood, *Solid State Commun.* **89**, 229 (1994)

[22] G Mariotto, E Cazzanelli, G Carturan, R Di Maggio and P Scardi, *J. Solid State Chem.* **86**, 263 (1990)

[23] S P S Porto and R S Krishnan, *J. Chem. Phys.* **17**, 1009 (1967)

[24] S Alexander and R Orbach, *J. Phys. Lett.* (*Paris*) **43**, L625 (1982)

[25] S Alexander, C Laermans, R Orbach and H M Rosenberg, *Phys. Rev.* **B28**, 4615 (1983)